HPLC Fractionation and Surface Micellization Behavior of Polystyrene-*b*-poly(methyl methacrylate)

Bonghoon Chung, Soojin Park, and Taihyun Chang*

Department of Chemistry and Center for Integrated Molecular Systems, Pohang University of Science and Technology, Pohang 790-784, Korea

Received April 11, 2005; Revised Manuscript Received May 16, 2005

ABSTRACT: A polystyrene-*block*-poly(methyl methacrylate) (PS-*b*-PMMA) was fractionated by HPLC, and the morphology of surface micelles formed at the air/water interface was investigated. Individual PS and PMMA blocks were fractionated by normal-phase and reversed-phase HPLC, respectively, into three fractions each to obtain nine fractions of narrower distribution in molecular weight as well as in composition. Although the mother PS-*b*-PMMA was prepared by anionic polymerization and had a narrow molecular weight distribution as characterized by size exclusion chromatography (M_w = 72.8 kg/mol, M_w/M_n = 1.08, PS wt % = 73.7%), the nine fractionated samples showed significant variations in molecular weight (M_w = 63.1−79.5 kg/mol) and in composition (PS wt % = 66.5−76.3%). The fractionated block copolymers formed more uniform surface micelles than the unfractionated mother PS-*b*-PMMA and exhibited a large variation with respect to the composition. The PS-*b*-PMMA fraction of the lowest PS content (66.5 wt %) showed circular micelles only. Rod-shaped micelles started to appear with a slight increase in the PS content, but circular and rod-shaped micelles coexist over ca. 10% concentration range and no sharp phase boundary appears to exist. The rod-shaped micelles formed at low PS contents exhibit a structure of linearly connected circular micelles.

Introduction

Block copolymers consist of different polymer chains connected by a chemical bond. If these blocks are not miscible each other, they can self-assemble to various microphase-separated morphologies on the nanometer scale. The microphase-separated bulk morphology has been studied extensively, and phase diagrams of different microphases are predicted theoretically and confirmed experimentally.[1−6] Such block copolymers also form micelles when dissolved in appropriate selective solvents.[7−9]

Amphiphilic block copolymers often form surface micelles when spread at the air/water interface. Since Zhu et al. first reported on the surface micelle morphology of polystyrene-*b*-poly(4-vinylpyridine) quaternized by alkyl iodide, a number of studies on various block copolymer surface micelles have been reported.[10−17] The shape of the surface micelles changes from circular micelles to large planar aggregates via rod-shaped micelles depending mainly on the relative size of the two blocks. Most block copolymers employed in these studies were prepared by sequential anionic polymerization that is the best available method to synthesize the polymers with narrow distributions in molecular weight as well as in composition. Nonetheless, the polymers have a small but finite dispersity in both molecular weight and composition.[18] In addition, the block copolymers often contain byproducts from the nonideal processes in the synthetic procedure. The most conspicuous byproduct in such block copolymers is the homopolymer precursor of the first block that was terminated when the second monomer was added for the polymerization of the second block.[19] Recently, Park et al. fractionated polystyrene-*block*-polyisoprene (PS-*b*-PI) diblock copolymers by HPLC to obtain the block copolymers with narrow distributions in molecular weight as well as in composition. They found that the fractions had a large variation in composition enough to exhibit several different bulk morphologies.[20,21]

The objective of this study is twofold. One is to find a good separation condition to fractionate the individual blocks of PS-*b*-PMMA by HPLC into the fractions having narrower distributions in both molecular weight and composition. We reported on the HPLC separation condition for PS-*b*-PI earlier,[20] but a suitable HPLC separation condition needs to be established for each different copolymer. The other is to learn how the polydispersity of the block copolymers would affect the surface micelle behavior. The finely divided fractions from a mother block copolymer would bring more detailed phase information on the surface micelles. While it has been well established that the morphology of the surface micelles depends on the block copolymer composition, the detailed phase behavior of the surface micelles is yet to be elucidated. For example, is the surface micelle formation similar to the microphase separation of block copolymers in bulk, in which sharp phase boundaries exist with respect to the composition of block copolymers? Would the surface micelle size become more homogeneous for the fractionated polymers?

Experimental Section

PS-*b*-PMMA was synthesized by sequential anionic polymerization of styrene and methyl methacrylate in THF at −78 °C under an Ar atmosphere. The details of the apparatus are described elsewhere.[22,23] The initiator was *sec*-BuLi (Aldrich), and 10 equiv of LiCl was added to suppress the side reaction in the polymerization of PMMA block.[24] The diblock copolymer was characterized by ^{1}H NMR spectroscopy (Bruker, DPX-300) for the composition and by size exclusion chromatography (SEC) for the molecular weight. For the SEC analysis, two polystyrene gel columns (Polymer Lab., PL-mixed C, 300 × 8 mm) were used in a column oven (Eppendorf, TC-50), and the

* Corresponding author: Tel +82-54-279-2109; Fax +82-54-279-3399; e-mail tc@postech.edu.

10.1021/ma050751r CCC: $30.25
Published on Web 06/14/2005

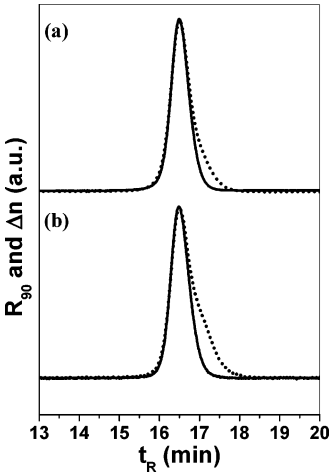

Figure 1. SEC chromatograms of as-prepared mother PS-*b*-PMMA (dotted lines) and homo-PS free mother PS-*b*-PMMA (solid lines) recorded by a light scattering (a) and a refractive index detector (b).

column temperature was kept at 40 °C. Mobile phase was THF at a flow rate of 0.8 mL/min. Chromatograms were recorded by a refractive index detector (Wyatt, Opti-Lab) and a multi-angle light scattering (MALS) detector (Wyatt, mini-Dawn).

HPLC Fractionation. HPLC apparatus consists of a solvent delivery pump (Polymer Lab., LC 1150), a six-port sample injector (Rheodyne 7125) equipped with a 100 μL injection loop, and an UV/vis absorption detector (Spectra-physics, Spectra Series, UV 100) operating at a wavelength of 260 nm. For the fractionation of PMMA block, a bare silica column (Nucleosil, 100 × 22 mm, 100 Å pore) and an isooctane/THF (35/65, v/v) mixture were used as the stationary and the mobile phase, respectively. For the fractionation of PS block, a reversed phase (RP) column (Nucleosil C18, 100 × 22 mm, 100 Å) and CH_2Cl_2/CH_3CN (54/46, v/v) mixture were used as the stationary and the mobile phase, respectively. The injection samples were prepared at a concentration of 120 mg/mL in the respective mobile phase solvents. The flow rate of the mobile phase was 1.8 mL/min.

Langmuir−Blodgett (LB) Film. Polymer solutions were prepared in chloroform (Mallinckrodt, HPLC grade) at a concentration of 0.5 mg/mL. Subphase of the LB trough (760 × 120 mm^2, KSV 5000, Helsinki, Finland) was deionized water (resistivity = 18.3 MΩ cm) prepared by a water purification system (Human, Korea). The subphase temperature was maintained at 23 ± 0.1 °C. After spreading the polymer solution, 15 min was allowed for complete evaporation of chloroform.

LB films were transferred on Si wafer at a vertical lift speed of 5 mm/min while maintaining the surface pressure at 7 mN/m. The Si wafers were pretreated with RCA method to clean the surface. The morphology of the LB films was investigated by a tapping mode AFM (Digital Instruments, Nanoscope III) equipped with 10 μm scanner and a silicon tip.

Result and Discussion

Figure 1 shows SEC chromatograms of the as-prepared PS-*b*-PMMA (solid line) and homo-PS free PS-*b*-PMMA (dashed line). As-prepared PS-*b*-PMMA shows a narrow and unimodal elution peak. The average molecular weight and the molecular weight distribution were calculated from the intensity of the light scattering and refractive index detectors. The composition of the block copolymer was determined by ^{1}H NMR from the ratio of the aryl proton signal intensity for PS (6−8 ppm) to the methoxy proton signal intensity for PMMA (~3.5 ppm). The block copolymer had a PS content of 73.7 wt %. The d*n*/d*c* value was determined by two different methods. One is the direct measurement using a differential refractometer. The other method is to calculate the d*n*/d*c* value from the composition of the block copolymers according to the following formula.

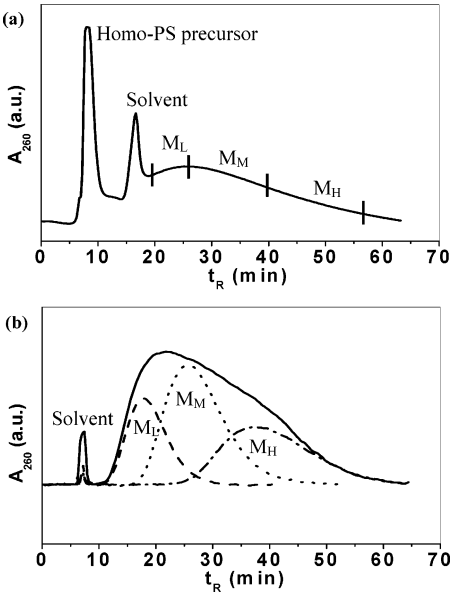

Figure 2. (a) NPLC chromatogram of the as-prepared PS-*b*-PMMA. Three fractions were collected over the regions as indicated with small vertical bars. (b) NPLC chromatograms of the homo-PS free PS-*b*-PMMA (solid line) and the three fractions (dashed line, M_L; dotted line, M_M; dash−dot line, M_H). Since the NPLC chromatograms (b) were obtained with an analytical column (250 × 4.6 mm), the retention time does not match with the chromatogram (a), which was obtained with a large bore column (100 × 22 mm) for the fractionation.

$$\mathrm{d}n/\mathrm{d}c = (\mathrm{d}n/\mathrm{d}c)_{\mathrm{PS}} w_{\mathrm{PS}} + (\mathrm{d}n/\mathrm{d}c)_{\mathrm{PMMA}} w_{\mathrm{PMMA}} \quad (1)$$

These two methods yielded the identical d*n*/d*c* value of 0.159 (d*n*/d*c* of PS and PMMA is 0.185 and 0.0875, respectively) within experimental precision. Thus, determined molecular weight and the molecular weight distributions are M_w = 72.8 kg/mol and M_w/M_n = 1.08, respectively. This SEC analysis result could have been regarded as a proof of a decent PS-*b*-PMMA prepared by anionic polymerization. The SEC chromatogram of the homo-PS free PS-*b*-PMMA will be discussed later.

Figure 2a displays a normal phase (NP) LC chromatogram of as-prepared PS-*b*-PMMA using a bare silica stationary phase. In this separation condition, PS homopolymers elute in the SEC region before the injection solvent peak. A significant amount of the homo-PS elutes at $t_R \approx 9$ min before the injection solvent peak eluting at $t_R \approx 18$ min. The homo-PS amounts about 14% of the total peak area, which corresponds to the fraction of homo-PS among the total amount of PS in the as-prepared PS-*b*-PMMA since PMMA does not absorb light at 260 nm wavelength. It may appear as if this PS-*b*-PMMA is not in good quality to contain such a high content of homo-PS precursors. However, we found the similar problems in many commercially available block copolymers, in particular for acrylate-containing polymers.[19] It is difficult to find the presence of homopolymer precursor in a block copolymer by SEC due to the low resolution of SEC, in particular if the molecular weight difference between the homopolymer precursor and the block copolymer is small (high content of the first block). Figure 1 compares the SEC chromatograms of the as-prepared PS-*b*-PMMA and the

homo-PS free PS-*b*-PMMA, which clearly demonstrate the incapability of SEC to detect the presence of homo-PS precursor.

Since the PMMA block interacts more strongly with the polar stationary phase, PS-*b*-PMMA is retained longer in the NP column than the homo-PS precursor and elutes after the injection solvent peak.[25] Since the retention changes very sensitively with the interaction strength, the elution peak is broad, indicating a rather broad distribution in the interaction strength (mainly due to the distribution in PMMA block length) of PS-*b*-PMMA. The broad NPLC elution peak of the as-prepared PS-*b*-PMMA was fractionated into three fractions at 1 °C. The collection ranges of the eluates are indicated with small vertical bars in Figure 2a. Since the interaction strength of PS-*b*-PMMA primarily depends on the PMMA block length, the fractions are labeled as M_L, M_M, and M_H, standing for the low, medium, and high molecular weight fractions of the PMMA block. Figure 2b displays the NPLC chromatograms of the three fractions together with the homo-PS free mother PS-*b*-PMMA. Since the NPLC chromatograms were obtained with an analytical column (Nucleosil, 250 × 4.6 mm, 100 Å pore, flow rate 0.5 min/mL), the retention time does not match with the chromatogram in Figure 2a, which was obtained with a large bore column for the fractionation. The disappearance of the homo-PS peak before the injection solvent peak eluting at $t_R \approx 7$ min ensures that the homo-PS is completely removed. The elution peaks of the three fractions are overlapped to some extent due to the band broadening in the large-scale fractionation, but it is apparent that their peak widths are narrowed down significantly.

The three fractions obtained from the NPLC fractionation were further fractionated by RPLC to fractionate the PS block selectively. Parts a, b, and c of Figure 3 show the RPLC chromatograms of the three NPLC fractions, M_L, M_M, and M_H, respectively. The three RPLC chromatograms were obtained at 35 (a), 37 (b), and 41 °C (c) to adjust the retention similarly. If the NPLC and RPLC retention depends exclusively on PMMA and PS block lengths, respectively, we should expect the identical RPLC chromatograms for M_L, M_M, and M_H without temperature adjustment. However, the RPLC retentions are not identical, indicating that the HPLC separations were not done exclusively, but mainly, for the corresponding blocks. The NPLC fractions were further fractionated into three fractions each, and the collection ranges are indicated with small vertical bars on the chromatograms. Again, the RPLC fractionated samples are coded as S_L, S_M, and S_H, indicating the low, medium, and high molecular weight of the PS block. The molecular characteristics of the nine fractions are summarized in Table 1.

First, we can note that the molecular weight and the composition of the homo-PS free PS-*b*-PMMA changed upon removal of the homo-PS to $M_w = 73.6$ kg/mol, $M_w/M_n = 1.05$, and 73.0 PS wt %. Table 1 shows that the individual blocks are indeed fractionated selectively as expected from the HPLC separation mechanisms, and the nine fractions show a significant composition variation. Each row shows a similar molecular weight for PMMA block (~17 kg/mol for M_L, ~20 kg/mol for M_M, and ~22 kg/mol for M_H) while each column shows a similar molecular weight for PS block (~45 kg/mol for S_L, ~50 kg/mol for S_M, and ~56 kg/mol for S_H). In

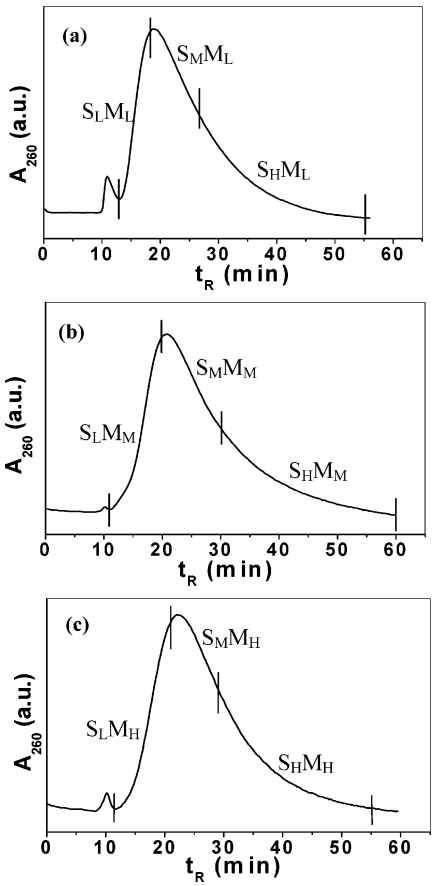

Figure 3. RPLC chromatograms of the three NPLC fractions, M_L, M_M, and M_H. They are obtained at the same separation condition except for the column temperatures: (a) 35, (b) 37, (c) 41 °C. The small vertical bars indicate the regions where the three fractions, S_L, S_M, and S_H were collected.

Table 1. Characterization Results of PS-*b*-PMMA Diblock Copolymers[a]

	NPLC fractionation	RPLC fractionation		
		S_L	S_M	S_H
M_w[b] (kg/mol)	M_L	63.1	67.7	72.3
M_w/M_n[c]		1.01	1.01	1.01
PS (wt %)[d]		73.1	75.6	76.3
M_w[b] (kg/mol)	M_M	64.8	69.5	77.6
M_w/M_n[c]		1.01	1.01	1.01
PS (wt %)[d]		68.5	72.1	74.1
M_w[b] (kg/mol)	M_H	65.3	71.3	79.5
M_w/M_n[c]		1.01	1.01	1.01
PS (wt %)[d]		66.5	69.9	71.1

[a] As-prepared mother PS-*b*-PMMA: $M_w = 72.8$ kg/mol, $M_w/M_n = 1.08$, 73.7 PS wt %. Homo-PS free mother PS-*b*-PMMA: $M_w = 73.6$ kg/mol, $M_w/M_n = 1.05$, 73.0 PS wt %. [b] Measured by SEC/MALS. [c] Determined by SEC/MALS. [d] Determined by ^{1}H NMR.

results, the nine fractions exhibit a significant difference in molecular weight as well as in composition. The largest difference in molecular weight can be found along the diagonal from S_LM_L ($M_w = 63.1$ kg/mol) to S_HM_H ($M_w = 79.5$ kg/mol), which amounts more than 20%. On the other hand, the largest difference in composition found along the diagonal from S_HM_L (PS wt % = 76.3%) to S_LM_H (PS wt % = 66.5%) amounts about 10%.

Block copolymer surface micelles are formed by spreading the chloroform solution of the block copolymers at the air/water interface. The AFM topography and phase image of the LB film of the homo-PS free PS-*b*-PMMA are displayed in Figure 4. The LB film was

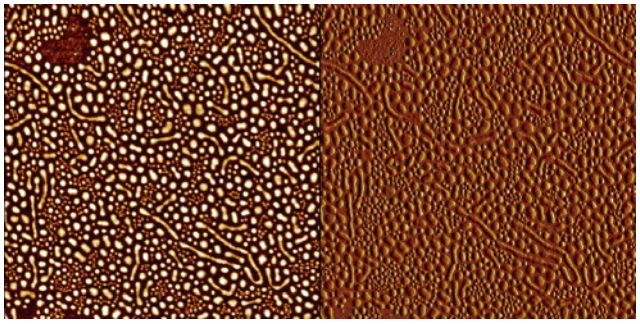

Figure 4. AFM topography and phase image (3 × 3 μm) of the LB film of the homo-PS free mother PS-*b*-PMMA block copolymer (left, height; right, phase mode). Though PS homopolymer was eliminated, morphology exhibited various form, such as small and large circular micelles and rod-shaped micelles. *Z* range: 9 nm; deposition pressure: 7 mN/m.

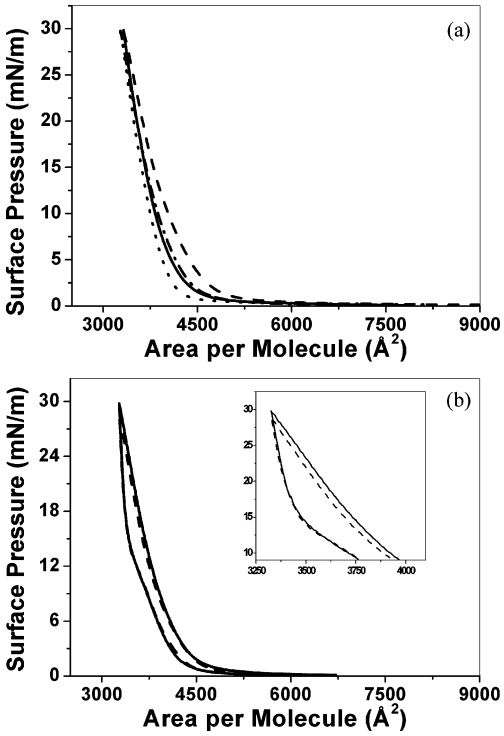

Figure 5. (a) Surface pressure−area isotherms of S_LM_H (dashed line), S_MM_M (dash−dot line), S_HM_L (dotted line), and homo-PS free mother PS-*b*-PMMA (solid line). (b) Surface pressure−area compression−expansion cycles for S_MM_M sample at 23 °C. In the inset, an expanded portion of the isotherm is displayed.

deposited on a silicon wafer at a surface pressure of 7 mN/m. At a higher deposition pressure, the transfer ratio of the LB film decreased seemingly due to the increase of the film rigidity. At a lower pressure, the number density of the surface micelle decreased while no significant change in the morphology was observed. Although the PS homopolymer was eliminated, the surface micelles exist in various forms, such as small and large circular micelles and rod-shaped micelles likely due to heterogeneity in molecular weight and composition of the polymer.

Figure 5a shows the surface pressure−area (π−A) diagram of the homo-PS free mother PS-*b*-PMMA and the three fractions (S_LM_H, S_MM_M, S_HM_L) of similar molecular weight while showing the largest contrast in the composition among the nine fractions. The π−A diagrams of the three fractions have similar shapes not much different from the homo-PS free mother PS-*b*-PMMA showing a condensed film behavior due to the short PMMA block.[26] The initial surface pressure was 0.2−0.3 mN/m when a 200 μL polymer solution was spread on the water subphase, and then the surface pressure does not change much upon initial compression. The surface pressure, however, increased rapidly from the point where the neighboring micelles start to interact each other. This is a typical behavior observed in surface micelles of block copolymer with short hydrophilic chain.[27]

The π−A diagrams of the three fractions show small but clearly distinguishable difference in π−A isotherms. The surface area per block copolymer molecule decreases in the order of S_LM_H (43.4K−21.9K), S_MM_M (50.1K−19.4K), and S_HM_L (55.2K−17.1K). It is not surprising that S_LM_H occupies the largest area among the three fractions despite the lowest total molecular weight since it has the longest, surface-active PMMA block. Because of the same reason, the compressibility of the monolayer (inversely proportional to the slope of the π−A isotherm) is in the order of $S_LM_H > S_MM_M > S_HM_L$. The compression−expansion cycles are shown for S_MM_M in Figure 5b. It shows a hysteresis behavior, but the compression and expansion cycles are nearly repeatable. The hysteresis loop is relatively small due to the short PMMA blocks but increases as the hydrophilic PMMA chain increased, which is consistent with the earlier finding with PS-*b*-PEO.[28,29]

The difference between the unfractionated and fractionated PS-*b*-PMMA can be found in the π−A diagrams, but more pronounced difference can be found in the morphology of the surface micelles as displayed in Figure 6. The fraction containing the least PS content (S_LM_H) shows only circular micelles of highly uniform size. Such a high uniformity of the surface micelles is evidently due to the high molecular uniformity in this fractionated diblock copolymer. All other fractions show mixed morphology of circular micelles and rod-shaped micelles, and the content of the rod-shaped micelles increases with the PS content. The largest variation of the morphology is observed along the diagonal from S_HM_L (PS wt % = 76.3%) to S_LM_H (PS wt % = 66.5%). For the other diagonal from S_LM_L to S_HM_H, along which the molecular weight varies most while the composition does not change much, surface micelle morphology does not show as much variation. This indicates that the surface micelle morphology is mainly controlled by the composition. To compare the morphologies in a more quantitative manner, we measure the number of circular and rod micelles and the average length of the rod micelles and summarize the results in Table 2. They are the average values measured from nine different 1 μm × 1 μm AFM images. The data show that not only the number but also the average length of the rod-shaped micelles increases as the PS content increases.

It is worthwhile to note that a small composition variation leads to a noticeable difference in micelle morphology. S_LM_H of the lowest PS content (66.5%) shows only circular micelles while S_LM_M, which has the second lowest PS content (68.5%), starts to show rod-shaped micelles, and the content of the rod-shaped micelles steadily increases as the PS content increases. The close examination of the rod-shaped micelles of S_LM_L reveals that they are actually the loosely connected linear arrays of the circular micelles as shown

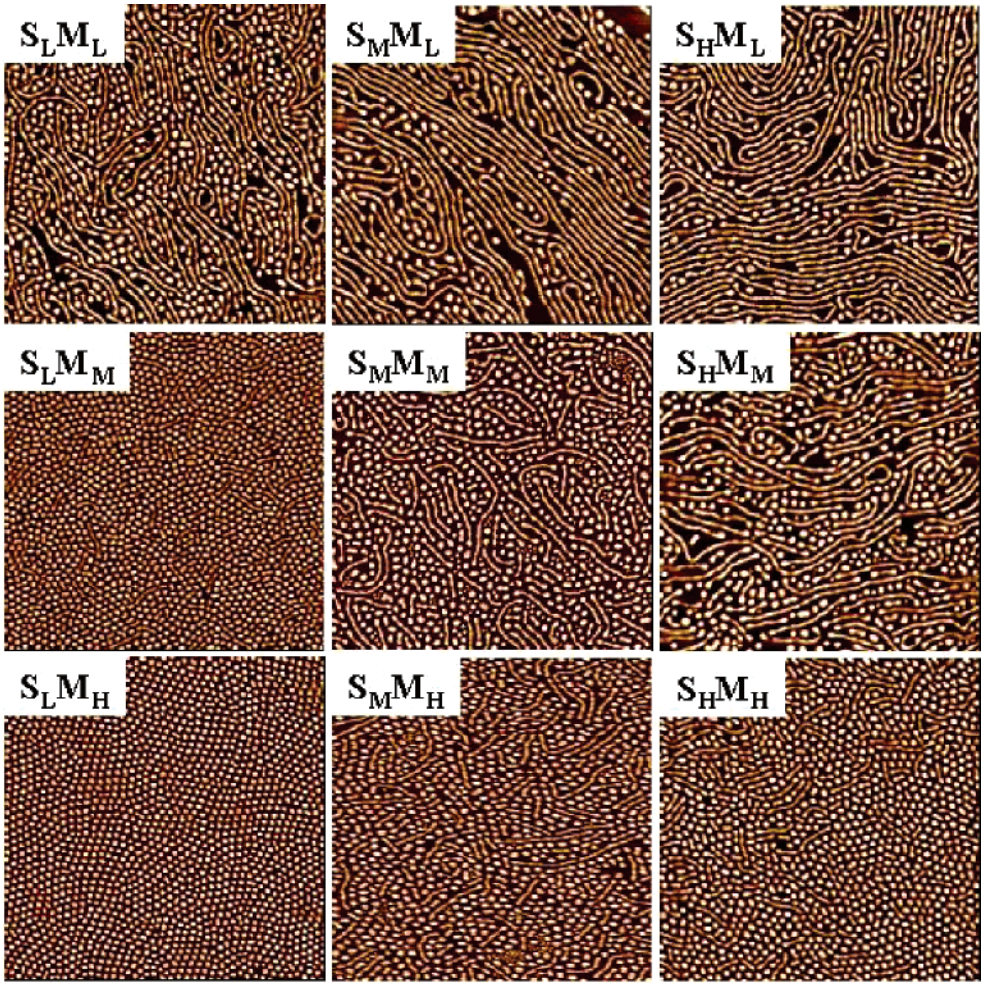

Figure 6. AFM topography images of the nine PS-*b*-PMMA fractions (3 μm × 3 μm). It clearly shows the trend in morphology change with the block copolymer composition.

Table 2. Statistics of the Surface Micelle Morphology[a]

NPLC: PMMA fractionation	RPLC: PS fractionation		
	S_L	S_M	S_H
M_L	17 ± 3[b]	20 ± 4	22 ± 2
	64 ± 6[c]	9 ± 3	10 ± 3
	1 μm[d]	2.5 μm	2.9 μm
M_M	7 ± 1	14 ± 5	19 ± 2
	205 ± 11	97 ± 8	41 ± 5
	0.5 μm	0.8 μm	2.1 μm
M_H	0	71	83
	214 ± 8	208 ± 8	165 ± 9
	0	0.5 μm	0.6 μm

[a] The values were averaged at nine different positions, and the uncertainty stands for one standard deviation. [b] Average number of rod micelles in 1 μm × 1 μm. [c] Average number of circular micelles in 1 μm × 1 μm. [d] Average length of rod micelles.

in Figure 7. This observation is consistent with the result of Seo et al.[26] Such a structure is maintained for the block copolymers with higher PS contents.

The two differently shaped micelles coexist over a wide composition range, and no sharp phase boundary appears to exist between the circular and rod-shaped micelle morphology. According to a theoretical study, a clear phase boundary may exist for this type of ultrathin films similar to the block copolymer bulk.[30] This discrepancy may reflect that the surface micelle morphology is not an equilibrium structure but affected significantly by kinetic effect. Devereaux et al. reported that surface micelle morphologies were affected by the factors other than the block copolymer composition such as concentration of spreading solution, compression speed, and deposition pressure.[27]

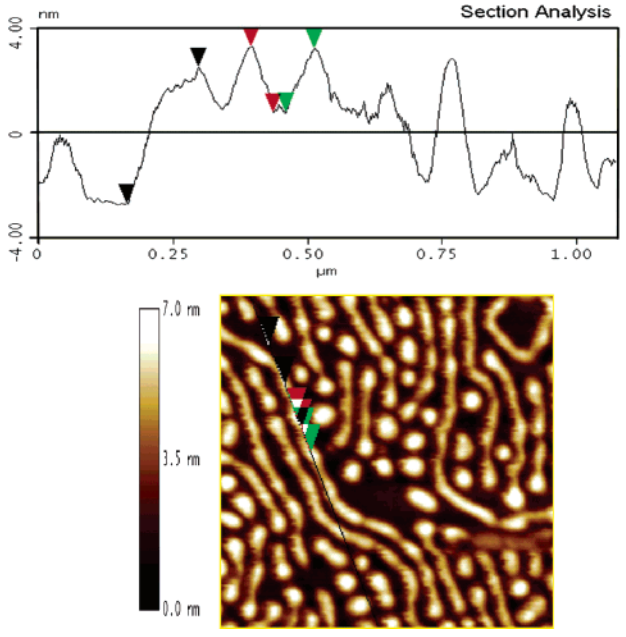

Figure 7. Height profile along a rod-shaped micelle in the AFM image of S_LM_L (1 μm × 1 μm). The height variation along the rod indicates that the rod is a loosely connected linear array of circular micelles.

In summary, HPLC separation conditions were established for the fractionation of individual blocks of PS-*b*-PMMA. In the course of HPLC fractionation, homo-PS precursors could be completely removed. By consecutive NPLC and RPLC fractionations, we obtained nine fractions having narrower dispersity in both molecular weight and composition. The fractions showed significant variations in composition (∼10%) and in molecular weight (∼20%).

The nine PS-*b*-PMMA fractions exhibited a more clearly developed surface micelle morphology than the unfractionated PS-*b*-PMMA, and the morphology depends sensitively on the block copolymer composition. At PS wt % = 66.5%, quite uniform circular micelles were observed from the fraction, which is evidently a result of the narrow dispersity of the fractionated block copolymers. A slight increase of the PS contents lead to the formation of rod-shaped micelles. The content of the rod-shaped micelles increases with the PS content, and there is no sharp boundary in composition exists between the two morphologies. The close examination of the rod-shaped micelles reveals that the micelles are linear aggregates of the circular micelles.

Acknowledgment. This study was supported by the research grants from KOSEF (Grant No. 951-0504-027-2 and the Center for Integrated Molecular Systems).

References and Notes

(1) Leibler, L. *Marcromolecules* **1980**, *13*, 1602.
(2) Fredrickson, G. H.; Helfand, E. *J. Chem. Phys.* **1987**, *87*, 697.
(3) Matsen, M. W.; Schick, M. *Macromolecules* **1994**, *27*, 4014.
(4) Hamley, I. W. *The Physics of Block Copolymers*; Oxford University Press: New York, 1998.
(5) Bates, F. S.; Fredrickson, G. H. *Phys. Today* **1999**, *52*, 32.
(6) Hashimoto, T. *Macromol. Symp.* **2001**, *174*, 69.
(7) Kotaka, T.; Tanaka, T.; Hattori, M.; Inagaki, H. *Macromolecules* **1978**, *11*, 138.
(8) Riess, G. *Prog. Polym. Sci.* **2003**, *28*, 1107.
(9) Foerster, S.; Zisenis, M.; Wenz, E.; Antonietti, M. *J. Chem. Phys.* **1996**, *104*, 9956.
(10) Zhu, J.; Eisenberg, A.; Lennox, R. B. *J. Am. Chem. Soc.* **1991**, *113*, 5583.
(11) Zhu, J.; Lennox, R. B.; Eisenberg, A. *J. Phys. Chem.* **1992**, *96*, 4727.
(12) Li, S.; Hanley, S.; Khan, I.; Varshney, S. K.; Eisenberg, A.; Lennox, R. B. *Langmuir* **1993**, *9*, 2243.
(13) Cox, J. K.; Yu, K.; Constantine, B.; Eisenberg, A.; Lennox, R. B. *Langmuir* **1999**, *15*, 7714.
(14) Gragson, D. E.; Jensen, J. M.; Baker, S. M. *Langmuir* **1999**, *15*, 6127.
(15) Baker, S. M.; Leach, K. A.; Devereaux, C. E.; Gragson, D. E. *Macromolecules* **2000**, *33*, 5432.
(16) Seo, Y.; Im, J. H.; Lee, J. S.; Kim, J. H. *Macromolecules* **2001**, *34*, 4842.
(17) Choi, M.; Chung, B.; Chun, B.; Chang, T. *Macromol. Res.* **2004**, *12*, 127.
(18) Tanaka, T.; Omoto, M.; Donkai, N.; Inagaki, H. *J. Macromol. Sci., Phys.* **1980**, *17*, 211.
(19) Park, S.; Park, I.; Chang, T.; Ryu, C. Y. *J. Am. Chem. Soc.* **2004**, *126*, 8906.
(20) Park, S.; Cho, D.; Ryu, J.; Kwon, K.; Lee, W.; Chang, T. *Macromolecules* **2002**, *35*, 5974.
(21) Park, S.; Kwon, K.; Cho, D.; Lee, B.; Ree, M.; Chang, T. *Macromolecules* **2003**, *36*, 4662.
(22) Ndoni, S.; Papadakis, C. M.; Bates, F. S.; Almdal, K. *Rev. Sci. Instrum.* **1995**, *66*, 1090.
(23) Kwon, K.; Lee, W.; Cho, D.; Chang, T. *Korea Polym. J.* **1999**, *7*, 321.
(24) Fayt, R.; Forte, R.; Jacobs, C.; Jerome, R.; T. Ouhadi; Teyssie, P.; Varshney, S. K. *Macromolecules* **1987**, *20*, 1442.
(25) Lee, W.; Cho, D.; Chun, B. O.; Chang, T.; Ree, M. *J. Chromatogr. A* **2001**, *910*, 51.
(26) Seo, Y.; Paeng, K.; Park, S. *Macromolecules* **2001**, *34*, 8735.
(27) Devereaux, C. A.; Baker, S. M. *Macromolecules* **2002**, *35*, 1921.
(28) Goncalves da Silva, A. M.; Gamboa, A. L. S.; Martinho, J. M. G. *Langmuir* **1998**, *14*, 5327.
(29) Goncalves da Silva, A. M.; Filipe, E. J. M.; d'Oliveira, J. M. R.; Martinho, J. M. G. *Langmuir* **1996**, *12*, 6547.
(30) Potemkin, I. I.; Kramarenko, E. Y.; Khokhlov, A. R.; Winkler, R. G.; Reineker, P.; Eibeck, P.; Spatz, J. P.; Moller, M. *Langmuir* **1999**, *15*, 7290.

MA050751R